

Histogram of Gradient Orientations of Signal Plots applied to P300 Detection

Rodrigo Ramele^{1,*}, Ana Julia Villar¹ and Juan Miguel Santos¹

¹*Centro de Inteligencia Computacional, Computer Engineering Department,
Instituto Tecnológico de Buenos Aires, Buenos Aires, Argentina*

Correspondence*:

Rodrigo Ramele, C1437FBH Lavarden 315, Ciudad Autónoma de Buenos Aires,
Argentina
rramele@itba.edu.ar

2 ABSTRACT

3 Word Count: ~~4841~~ 4961

4 The analysis of Electroencephalographic (EEG) signals is of ulterior importance for decoding
5 patterns that could improve the implementation of Brain Computer Interfaces (BCI). These
6 systems are meant to provide alternative pathways to transmit volitional information which could
7 potentially enhance the quality of life of patients affected by neurodegenerative disorders and
8 other mental illness. Of particular interests are those which are based on the recognition of
9 Event-Related Potentials (ERP) because they can be elicited by external stimuli and used to
10 implement spellers, to control external devices or even avatars in virtual reality environments.
11 This work mimics what electroencephalographers have been doing clinically, visually inspecting
12 and categorizing phenomena within the EEG by the extraction of features from images of signal
13 plots. It also aims to provide a framework to analyze, characterize and classify EEG signals, with
14 a focus on the P300, an ERP elicited by the oddball paradigm of rare events. The validity of the
15 method is shown by offline processing a public dataset of Amyotrophic Lateral Sclerosis (ALS)
16 patients and an own dataset of healthy subjects.

17 **Keywords:** **electroencephalography, histogram of gradient orientations, brain-computer interfaces, P300, SIFT, amyotrophic lateral**
18 **sclerosis, naive-bayes near neighbours, waveforms**

1 INTRODUCTION

19 Although recent advances in neuroimaging techniques, particularly radio-nuclear and radiological
20 scanning methods (?), have diminished the prospects of the traditional Electroencephalography (EEG),
21 the advent and development of digitized devices has impelled for a revamping of this hundred years old
22 technology. Their versatility, ease of use, temporal resolution, ease of development and production, and
23 its proliferation as consumer devices, are pushing EEG to become the de-facto non invasive portable or
24 ambulatory method to access and harness brain information (?).

25 A key contribution to this expansion has been the field of Brain Computer Interfaces (BCI) (?) which is
26 the pursuit of the development of a new channel of communication particularly aimed to persons affected
27 by neurodegenerative diseases.

28 One noteworthy aspect of this novel communication channel is the ability to transmit information from
29 the Central Nervous System (CNS) to a computer device and from there use that information to control a
30 wheelchair (?), as input to a speller application (?), in a Virtual Reality environment (?) or as aiding tool
31 in a rehabilitation procedure (?). The holly grail of BCI is to implement a new complete and alternative
32 pathway to restore lost locomotion (?).

33 EEG signals are remarkably complex and have been characterized as a multichannel non-stationary
34 stochastic process. Additionally, they have high variability between different subjects and even between
35 different moments for the same subject, requiring adaptive and co-adaptive calibration and learning
36 procedures (?). Hence, this imposes an outstanding challenge that is necessary to overcome in order to
37 extract information from raw EEG signals.

38 BCI has gained mainstream public awareness with worldwide challenge competitions like Cybathlon (??)
39 and even been broadcasted during the inauguration ceremony of the 2014 Soccer World Cup. New
40 developments have overcome the out-of-the-lab high-bar and they are starting to be used in real world
41 environments (??). However, they still lack the necessary robustness, and its performance is well behind
42 any other method of human computer interaction, including any kind of detection of residual muscular
43 movement (?).

44 A few works have explored the idea of exploiting the signal waveform to analyze the EEG signal.
45 In (?) an approach based on Slope Horizontal Chain Code is presented, whereas in (?) a similar
46 procedure was implemented based on Mathematical Morphological Analysis. The seminal work of Bandt-
47 Pompe Permutation Entropy (?) also explores succinctly this idea as a basis to establish the time series
48 ordinal patterns. In the article (?), the authors introduce a method for classification of rhythmic EEG
49 events like Visual Occipital Alpha Waves and Motor Imagery Rolandic Central μ Rhythms using the
50 histogram of gradient orientations of signal plots. Inspired in that work, we propose a novel application
51 of the developed method to classify and describe transient events, particularly the P300 Event Related
52 Potential. The proposed approach is based on the waveform analysis of the shape of the EEG signal, but
53 using histogram of gradient orientations. The method is built by mimicking what ~~traditionally~~ regularly
54 electroencephalographers have been performing for almost a century as it is described in (?): visually
55 inspecting raw signal plots.

56 This paper reports a method to, (1) describe a procedure to capture the shape of a waveform of an ERP
57 component, the P300, using histograms of gradient orientations extracted from images of signal plots, and
58 (2) outline the way in which this procedure can be used to implement an offline P300-based BCI Speller
59 application. Its validity is verified by offline processing two datasets, one of data from ALS patients and
60 another one from data of healthy subjects.

61 This article unfolds as follows: Section 2.1 is dedicated to explain the Feature Extraction method based
62 on Histogram of Gradient Orientations of the Signal Plot: Section 2.1.1 shows the preprocessing pipeline,
63 Section 2.1.2 describes the image generation of the signal plot, Section 2.1.3 presents the feature extraction
64 procedure while Section 2.1.4 introduces the Speller Matrix Letter Identification procedure. In Section 2.2,
65 the experimental protocol is expounded. Section 3 shows the results of applying the proposed technique. In
66 the final Section 4 we expose our remarks, conclusions and future work.

2 MATERIALS AND METHODS

67 The P300 (??) is a positive deflection of the EEG signal which occurs around 300 ms after the onset of a
68 rare and deviant stimulus that the subject is expected to attend. It is produced under the oddball paradigm (?)

and it is consistent across different subjects. It has a lower amplitude ($\pm 5\mu V$) compared to basal EEG activity, reaching a Signal to Noise Ratio (SNR) of around -15 db estimated based on the amplitude of the P300 response signal divided by the standard deviation of the background EEG activity (?). This signal can be used to implement a speller application by means of a Speller Matrix (?). Fig. This matrix is composed of 6 rows and 6 columns of numbers and letters. The subject can focus on one character of the matrix. Figure 1 shows an example of the Speller Matrix used in the OpenVibe open source software (?), where the flashes of rows and columns provide the deviant stimulus required to elicit this physiological response. Each time a row or a column that contains the desired letter flashes, the corresponding synchronized EEG signal should also contain the P300 signature and by detecting it, the selected letter can be identified.

2.1 Feature Extraction from Signal Plots

In this section, the signal preprocessing, the method for generating images from signal plots, the feature extraction procedure and the Speller Matrix identification are described. Figure 2 shows a scheme of the entire process.

2.1.1 Preprocessing Pipeline

The data obtained by the capturing device is digitalized and a multichannel EEG signal is constructed, where rows are sample points and columns are channels (electrodes).

The 6 rows and 6 columns of the Speller Matrix are intensified providing the visual stimulus. The number of a row or column is a location. A sequence of twelve randomly permuted locations l conform an intensification sequence. The whole set of twelve intensifications is repeated k_a times.

- **Signal Enhancement:** The preprocessing stage consists of the enhancement of the SNR of the P300 pattern above the level of basal EEG. The pipeline starts by applying a notch filter to the raw digital signal, a 4th degree 10 Hz lowpass Butterworth filter and finally a decimation with a Finite Impulse Response (FIR) filter of order 30 from the original sampling frequency down to 16 Hz (?).
- **Artifact Removal:** The multichannel EEG signal is processed on a channel by channel basis. For every complete sequence of 12 intensifications of 6 rows and 6 columns, a basic artifact elimination procedure is implemented by removing the entire sequence when any signal deviates above/below $\pm 70\mu V$.
- **Segmentation:** For each of the 12 intensifications, a window of one intensification sequence, a segment S_i^l of a window of t_{max} seconds of $t_{max} = 1$ second of the multichannel signal is extracted, starting from the stimulus onset, corresponding to each row/column intensification l and to the intensification sequence i . As intensifications are permuted in a random order, the segments are rearranged corresponding to row flickering, labeled 1-6, whereas those corresponding to column flickering are labeled 7-12. Two of these segments should contain the P300 ERP signature time-locked to the flashing stimulus, one for the row, and one for the column.
- **Signal Averaging:** The P300 ERP is deeply buried under background basal EEG so the traditional standard approach to identify it is by point-to-point averaging the time-locked stacked signal segments. Hence the values which are not related to, and not time-locked to the onset of the stimulus are canceled out (?).

This last step determines the operation of any P300 Speller. In order to obtain an improved signal in terms of its SNR, repetitions of the sequence of row/column intensification are necessary. And, at the same time, as long as more repetitions are needed, the ability to transfer information faster is diminished, so there is a trade-off that must be acutely determined.

111 2.1.2 Ensemble Average

112 The procedure to obtain the point-to-point averaged signal goes as follows:

- 113 1. Highlight randomly the rows and columns from the matrix. There is one row and one column that
114 should match the letter selected by the subject.
- 115 2. Repeat step 1 k_a times, obtaining the ~~single trial segments~~ $S_1(n, c), \dots, S_{k_a}(n, c)$ $1 \leq l \leq 12$
116 ~~segments~~ $S_1^l(n, c), \dots, S_{k_a}^l(n, c)$, of the EEG signal where the variables $n \in \{1, \dots, n_{max}\}$ and
117 $c \in \{1, 2, \dots, Ch\}$ $1 \leq n \leq n_{max}$ and $1 \leq c \leq C$ correspond to sample points and channel,
118 respectively. The parameter $Ch - C$ is the number of available EEG channels whereas
119 $n_{max} = F_s \cdot t_{max}$ $n_{max} = F_s \cdot t_{max}$ is the segment length and F_s is the sampling frequency. The
120 parameter k_a is the number of repetitions of intensifications and it is an input parameter of the
121 algorithm.
- 122 3. Compute the Ensemble Average by

$$x^l(n, c) = \frac{1}{k_a} \sum_{i=1}^{k_a} S_i^l(n, c), \quad n \in \{1, n_{max}\}, c \in \{1, Ch\} \quad (1)$$

123 for each row and column on the Speller Matrix. $1 \leq n \leq n_{max}$ and for the channels $1 \leq c \leq C$.
124 This provide an averaged signal $x^l(n, c)$ for the twelve locations $1 \leq l \leq 12$.

125 2.1.2 Signal Plotting

126 Averaged signal segments are standardized and scaled for $1 \leq n \leq n_{max}$ and $1 \leq c \leq C$ by

$$\tilde{x}^l(n, c) = \left[\gamma \cdot \frac{(x(n, c) - \bar{x}(c))}{\hat{\sigma}(c)} \right] \frac{(x^l(n, c) - \bar{x}^l(c))}{\hat{\sigma}^l(c)}, \quad n \in \{1, n_{max}\}, c \in \{1, 2, Ch\} \quad (2)$$

where $\gamma > 0$ is an input parameter of the algorithm and it is related to the image scale. In addition, $x(n, c)$ is the point-to-point averaged multichannel EEG signal for the sample point n and for channel c . Lastly,

$$\bar{x}^l(c) = \frac{1}{n_{max}} \sum_{n=1}^{n_{max}} x^l(n, c)$$

and

$$\hat{\sigma}^l(c) = \left(\frac{1}{n_{max} - 1} \sum_{n=1}^{n_{max}} (x^l(n, c) - \bar{x}^l(c))^2 \right)^{\frac{1}{2}}$$

127 are the mean and estimated standard deviation of $x(n, c), n \in \{1, \dots, n_{max}\}$ $x^l(n, c), 1 \leq n \leq n_{max}$, for
128 each channel c .

129 Consequently, the image is constructed by placing the sample points for a pixel (z_1, z_2) , the image $I^{(l,c)}$
130 is constructed according to

$$I^{(l,c)}(z_1, z_2) = \begin{cases} 255 & \text{if } z_1 = \gamma n; z_2 = \tilde{x}^l(n, c) + z^l(c) \\ 0 & \text{otherwise} \end{cases} \quad (3)$$

131 where $(z_1, z_2) \in \mathbb{N} \times \mathbb{N}$ iterate over the width (based on the length of the signal segment) and height (based
 132 on the peak-to-peak amplitude) of the newly created image, $n \in \{1, \dots, n_{max}\}$ and $c \in \{1, 2, \dots, Ch\}$.
 133 The values $z(c)$, $c \in \{1, 2, \dots, Ch\}$ are the location on the image with $1 \leq n \leq n_{max}$ and $1 \leq c \leq C$.
 134 The value $z^l(c)$ is the image vertical position where the signal's zero value has to be located situated in
 135 order to fit the entire signal within the image for each channel c :

$$z^l(c) = \left\lfloor \frac{\max_n \tilde{x}(n, c) - \min_n \tilde{x}(n, c)}{2} \frac{\max_n \tilde{x}^l(n, c) - \min_n \tilde{x}^l(n, c)}{2} \right\rfloor - \left\lfloor \frac{\max_n \tilde{x}(n, c) + \min_n \tilde{x}(n, c)}{2} \frac{\max_n \tilde{x}^l(n, c) + \min_n \tilde{x}^l(n, c)}{2} \right\rfloor \quad (4)$$

136 where the minimization and maximization are carried out for n varying between $1 \leq n \leq n_{max}$, and $\lfloor \cdot \rfloor$
 137 denote the rounding to the smaller nearest integer of the number.

138 In order to complete the plot $I^{(l,c)}$ from the pixels, the Bresenham (?) algorithm is used to interpolate
 139 straight lines between each pair of consecutive pixels.

140 2.1.3 Feature Extraction: Histogram of Gradient Orientations

141 On the generated image $I^{(l,c)}$ For each generated image $I^{(l,c)}$, a keypoint \mathbf{kp}_p is placed on a pixel (x_{kp}, y_{kp})
 142 (x_{pk}, y_{pk}) over the image plot and a window around the keypoint is considered. A local image patch of size
 143 $S_p \times S_p$ pixels is constructed by dividing the window in 16 blocks of size $3s$ each one, where s
 144 is the scale of the local patch and it is an input parameter of the algorithm. It is arranged in a 4×4 grid and
 145 the pixel \mathbf{kp}_p is the patch center, thus $S_p = 12s$ $X_p = 12s$ pixels.

146 A local representation of the signal shape within the patch can be described by obtaining the gradient
 147 orientations on each of the 16 blocks $B_{i,j}$ with $0 \leq i, j \leq 3$ and creating a histogram of gradients. This
 148 technique is based on Lowe's SIFT (?) method, and it is biomimetically inspired in how the visual cortex
 149 detects shapes by analyzing orientations (?). In order to calculate the histogram, the interval $[0, 360]$
 150 $[0, 360]$ of possible angles is divided in 8 bins, each one at 45 degrees.

151 Hence, for each spacial bin $i, j = \{0, 1, 2, 3\}$ spatial bin $0 \leq i, j \leq 3$, corresponding to the indexes of
 152 each block $B_{i,j}$, the orientations are accumulated in a 3-dimensional histogram h through the following
 153 equation:

$$h(\theta, i, j) = 3s \sum_{\mathbf{p} \in I^{(l,c)}} w_{ang}(\angle J(\mathbf{p}) - \theta) w_{ij} \left(\frac{\mathbf{p} - \mathbf{kp}}{3s} \frac{\mathbf{p} - \mathbf{pk}}{3s} \right) |J(\mathbf{p})| \quad (5)$$

154 where \mathbf{p} is a pixel from the image $I^{(l,c)}$, θ is the angle bin with $\theta \in$
 155 $\{0, 45, 90, 135, 180, 225, 270, 315\}$, $|J(\mathbf{p})|$ is the norm of the gradient vector in the pixel \mathbf{p} and it is
 156 computed using finite differences and $\angle J(\mathbf{p})$ is the angle of the gradient vector. The scalar $w_{ang}(\cdot)$ and
 157 vector $w_{ij}(\cdot)$ functions are linear interpolations used by ? and ? to provide a weighting contribution to
 158 eight adjacent bins. They are calculated as

$$w_{ij}(\mathbf{v}) = w(v_x - x_i)w(v_y - y_{ij}) \quad (6)$$

$$w_{\text{ang}}(\alpha) = \sum_k w\left(\frac{8\alpha}{2\pi} + 8r\right)$$

159 with $0 \leq i, j \leq 3$ and

$$w_{\text{ang}}(\alpha) = \sum_{r=-1}^1 w\left(\frac{8\alpha}{2\pi} + 8r\right) \quad (7)$$

160 where x_i and y_i are the spatial bin centers located in $x_i, y_i = \{-\frac{3}{2}, -\frac{1}{2}, \frac{1}{2}, \frac{3}{2}\}$, $x_i, y_i \in \{-\frac{3}{2}, -\frac{1}{2}, \frac{1}{2}, \frac{3}{2}\}$,
 161 $\mathbf{v} = (v_x, v_y)$ is a dummy vector variable and α a dummy scalar variable. On the other hand, r is an integer
 162 that can vary freely between $[-1, 1]$ which allows the argument α to be unconstrained in terms of its values
 163 in radians. The interpolating function $w(\cdot)$ is defined as $w(z) = \max(0, |z| - 1)$.

$$w(z) = \max(0, |z| - 1)$$

164 These binning functions conform a trilinear interpolation that has a combined effect of sharing the
 165 contribution of each oriented gradient between their eight adjacent bins in a tridimensional cube in the
 166 histogram space, and zero everywhere else.

167 Lastly, the fixed value of 3 is a magnification factor which corresponds to the number of pixels per each
 168 block when $s = 1$. As the patch has 16 blocks and 8 bin angles are considered, for each location l and
 169 channel c a feature called descriptor $\mathbf{d}^{(l,c)}$ of 128 dimension is obtained.

170 Fig. 3 shows an example of a patch and a scheme of the histogram computation. In (A) a plot of
 171 the signal and the patch centered around the keypoint is shown. In (B) the possible orientations on each
 172 patch are illustrated. Only the upper-left four blocks are visible. The first eight orientations of the first
 173 block, are labeled from 1 to 8 clockwise. The orientations of the second block $B_{1,2}$ are labeled from 9 to
 174 16. This labeling continues left-to-right, up-down until the eight orientations for all the sixteen blocks are
 175 assigned. They form the corresponding kp-descriptor descriptor \mathbf{d} of 128 coordinates. Finally, in (C) an
 176 enlarged image plot is shown where the oriented gradient vector for each pixel can be seen.

177 2.1.4 Speller Matrix letter Identification

178 The aim is to identify the selected letter from the matrix. Previously, during the training phase, two
 179 descriptors are extracted from averaged signal segments which correspond to the letter where the user was
 180 supposed to be focusing onto. These descriptors are the P300 templates which are grouped in a template
 181 set called T . This set is constructed using the steps described in Section 2.1.1 and the steps A and B of the
 182 following algorithm.

183 2.1.4.1 P300 ERP Extraction

184 Segments corresponding to rows-row flickering are labeled 1-6, whereas those corresponding to columns
 185 column flickering are labeled 7-12. The whole extraction process has the following steps:

186 First highlight randomly the

- **Step A:** First highlight rows and columns from the matrix in a random permutation order and obtain the Ensemble Average as detailed in steps 1, 2 and 3 in Section 2.1.1.
- **Step AB:** Plot the signals $x(n, e)$, $n \in \{1, \dots, n_{max}\}$, $e \in \{1, \dots, Ch\}$ $\tilde{x}^l(n, c)$, $1 \leq n \leq n_{max}$, $1 \leq c \leq C$, according Section 2.1.2 in order to generate the images $I_1^{row}, \dots, I_6^{row}$ and $I_7^{col}, \dots, I_{12}^{col}$ $I^{(l,c)}$ for rows and columns, respectively $1 \leq l \leq 12$.
- **Step BC:** Obtain the descriptors $d_1^{row}, \dots, d_6^{row}$ and $d_7^{col}, \dots, d_{12}^{col}$ $\mathbf{d}^{(l,c)}$ for rows and columns, respectively from $I_1^{row}, \dots, I_6^{row}$ and $I_7^{col}, \dots, I_{12}^{col}$ from $I^{(l,c)}$ in accordance to the method described in Section 2.1.3.

2.1.4.2 Calibration

A trial, as defined by the BCI2000 platform (?), is every attempt to select just one letter from the speller. A set of trials is used for calibration and once the calibration is complete it can be used to identify new letters from new trials.

During the calibration phase, two descriptors $\mathbf{d}^{(l,c)}$ are extracted for each available channel, corresponding to the locations l of a selection of one previously instructed letter from the set of calibration trials. These descriptors are the P300 templates, grouped together in a template set called T^c . The set is constructed using the steps described in Section 2.1.1 and the steps A, B and C of the P300 ERP extraction process.

Additionally, the best performing channel, bpc is identified based on the the channel where the best Character Recognition Rate is obtained.

2.1.4.3 Letter identification

In order to identify the selected letter, the template set T^{bpc} is used as a database. Thus, new descriptors are computed and they are compared against the descriptors belonging to the calibration template set T^{bpc} .

- **Step CD:** Match to the Template T calibration template T^{bpc} by computing

$$\hat{row} = \arg \min_{u \in \{1, \dots, 6\}} \sum_{l \in \{1, \dots, 6\}} \sum_{q \in NN_T(d_u^{row})} \left\| q - d_u^{row} \mathbf{d}^{(l,bpc)} \right\| \quad (8)$$

and

$$\hat{col} = \arg \min_{u \in \{7, \dots, 12\}} \sum_{l \in \{7, \dots, 12\}} \sum_{q \in NN_T(d_u^{col})} \left\| q - d_u^{col} \mathbf{d}^{(l,bpc)} \right\| \quad (9)$$

where $NN_T(d_u^l)$, $l \in \{row, col\}$ is the set of the k nearest neighbors to d_u^l and q is a template descriptor that belongs to it. $N_T(\mathbf{d}^{(l,bpc)})$ is defined as $N_T(\mathbf{d}^{(l,bpc)}) = \{\mathbf{d} \in T^{bpc} / \mathbf{d}$ is the k -nearest neighbor of $\mathbf{d}^{(l,bpc)}\}$ for the best performing channel. This set is obtained by sorting all the elements in T based on the T^{bpc} based on distances between them and $d_u^l \mathbf{d}^{(l,bpc)}$, choosing the k smaller elements with smaller values, with k a parameter of the algorithm. This procedure is a modification of based on the k-NBNN algorithm (?).

By computing the aforementioned equations, the letter of the matrix can be determined from the intersection of the row \hat{row} and column \hat{col} . Figure 2 shows a scheme of this process.

220 2.2 Experimental Protocol

221 To verify the validity of the proposed framework and method, the public dataset 008-2014 (?) published
222 on the BNCI-Horizon website (?) by IRCCS Fondazione Santa Lucia, is used. Additionally, an own dataset
223 with the same experimental conditions is generated. Both of them are utilized to perform an offline BCI
224 Simulation to decode the spelled words from the provided signals.

225 The algorithm is implemented using VLFeat (?) Computer Vision libraries on MATLAB V2014a
226 (Mathworks Inc., Natick, MA, USA). Furthermore, in order to enhance the impact of our paper and for a
sake of reproducibility, the code of the algorithm has been made available at: <https://bitbucket.org/itba/hist>.
227
228

229 In the following sections the characteristics of the datasets and parameters of the identification algorithm
230 are described.

231 2.2.1 P300 ALS Public Dataset

232 The experimental protocol used to generate this dataset is explained in (?) but can be summarized as
233 follows: 8 subjects with confirmed diagnoses but on different stages of ALS disease, were recruited and
234 accepted to perform the experiments. The Visual P300 detection task designed for this experiment consisted
235 of spelling 7 words of 5 letters each, using the traditional P300 Speller Matrix (?). The flashing of rows
236 and columns provide the deviant stimulus required to elicit this physiological response. The first 3 words
237 are used for training calibration and the remaining 4 words, for testing with visual feedback. A trial, as
defined by the BCI2000 platform (?), is every attempt to select a letter from the speller. It is composed
238 of signal segments corresponding to $k_a = 10$ repetitions of flashes of 6 rows and $k_a = 10$ repetitions of
239 flashes of 6 columns of the matrix, yielding 120 repetitions. Flashing of a row or a column is performed for
240 0.125 s, following by a resting period (i.e. inter-stimulus interval) of the same length. After 120 repetitions
241 an inter-trial pause is included before resuming with the following letter.

243 The recorded dataset was sampled at 256 Hz and it consisted of a scalp multichannel EEG signal for
244 electrode channels Fz, Cz, Pz, Oz, P3, P4, PO7 and PO8, identified according to the 10-20 International
245 System, for each one of the 8 subjects. The recording device was a research-oriented digital EEG device
246 (g.Mobilab, g.Tec, Austria) and the data acquisition and stimuli delivery were handled by the BCI2000
247 open source software (?).

248 In order to assess and verify the identification of the P300 response, subjects are instructed to perform a
249 copy-spelling task. They have to fix their attention to successive letters for copying a previously determined
250 set of words, in contrast to a free-running operation of the speller where each user decides on its own what
251 letter to choose.

252 2.2.2 P300 for healthy subjects

253 We replicate the same experiment on healthy subjects (?) using a wireless digital EEG device (g.Nutilus,
254 g.Tec, Austria). The experimental conditions are the same as those used for the previous dataset, as detailed
255 in section 2.2.1. The produced dataset is available in a public online repository (?).

256 Participants are recruited voluntarily and the experiment is conducted anonymously in accordance with
257 the Declaration of Helsinki published by the World Health Organization. No monetary compensation
258 is handed out and all participants agree and sign a written informed consent. This study is approved
259 by the *Departamento de Investigación y Doctorado, Instituto Tecnológico de Buenos Aires (ITBA)*. All
260 healthy subjects have normal or corrected-to-normal vision and no history of neurological disorders. The

261 experiment is performed with 8 subjects, 6 males, 2 females, 6 right-handed, 2 left-handed, average age
 262 29.00 years, standard deviation 11.56 years, range 20-56 years.

263 EEG data is collected in a single recording session. Participants are seated in a comfortable chair, with
 264 their vision aligned to a computer screen located one meter in front of them. The handling and processing
 265 of the data and stimuli is conducted by the OpenVibe platform (?).

266 Gel-based active electrodes (g.LADYbird, g.Tec, Austria) are used on the same ~~locations~~positions Fz,
 267 Cz, Pz, Oz, P3,P4, PO7 and PO8. Reference is set to the right ear lobe and ground is preset as the AFz
 268 position. Sampling frequency is slightly different, and is set to 250 Hz, which is the closest possible to the
 269 one used with the other dataset.

270 2.2.3 Parameters

271 The patch size is $S_P = 12s \times 12s$ $X_P = 12s \times 12s$ pixels, where s is the scale of the local patch and it
 272 is an input parameter of the algorithm. The P300 event can have a span of 400 ms and its amplitude can
 273 reach $10\mu V$ (?). Hence it is necessary to utilize a ~~size patch~~ S_P signal segment of size $t_{max} = 1$ second
 274 and a size patch X_P that could capture an entire transient event. With this purpose in consideration, the s
 275 value election is essential.

276 We propose the Equations 10 and 11 to compute the scale value in horizontal and vertical directions,
 277 respectively.

$$s_x = \frac{\lambda \cdot F_s}{12} \cdot \gamma \frac{\Delta \mu V}{12} \quad (10)$$

$$s_y = \frac{\Delta \mu V}{12} \cdot \gamma \frac{\Delta \mu V}{12} \quad (11)$$

278 where λ is the length in seconds covered by the patch, F_s is the sampling frequency of the EEG
 279 signal (downsampled to 16 Hz) and $\Delta \mu V$ corresponds to the amplitude in microvolts that can be covered
 280 by the height of the patch. The geometric structure of the patch forces a squared configuration, then
 281 we discerned that by using $s = s_x = s_y = 3$ and $\gamma = 4$, the local patch and the descriptor can
 282 identify events of $9 \mu V$ of amplitude, with a span of $\lambda = 0.56$ seconds. This also determines that 1
 283 pixel represents $\frac{1}{\gamma} = \frac{1}{4} \mu V$ on the vertical direction and $\frac{1}{F_s \cdot \gamma} = \frac{1}{64} \frac{1}{F_s} = \frac{1}{64}$ seconds on the horizontal
 284 direction. ~~Descriptors~~ k_p The keypoints p_k are located at $(x_{kp}, y_{kp}) = (0.55F_s \cdot \gamma, z(e)) = (35, z(e))$
 285 $(x_{pk}, y_{pk}) = (0.55F_s \cdot \gamma, z^l(c)) = (35, z^l(c))$ for the corresponding channel c and location l (see Eq. 4).
 286 In this way the whole transient event is captured. Figure 4 shows a patch of a signal plot covering the
 287 complete amplitude (vertical direction) and the complete span of the signal event (horizontal direction).

288 Lastly, the number of channels C_h is equal to 8 for both datasets, and the number of
 289 intensification sequences k_a is ~~statically assigned fixed~~ to 10. The parameter k used to construct the
 290 set $NN_T(d_u^l), l \in \{row, col\}$ $N_T(d^{(l,c)})$ is assigned to $k = 7$, which was found empirically to achieve
 291 better results. In addition, the norm used on Equations 8 and 9 is the cosine norm, and descriptors are
 292 normalized to $[-1, 1]$.

3 RESULTS

293 Table 22-1 shows the results of applying the algorithm to the subjects of the public dataset of ALS patients.
 294 The percentage of correctly spelled letters is calculated while performing an offline BCI Simulation. From

295 the seven words for each subject, the first three are used as training calibration, and the remaining four
296 for testing. The best performing channel bpc is informed as well. The target ratio is 1 : 36; hence chance
297 level is 2.8%. It can be observed that the best performance of the letter identification method is reached in
298 various channels a dissimilar channel depending on the subject been studied.

299 The Information Transfer Rate (ITR), or Bit Transfer Rate (BTR), in the case of reactive BCIs (?)
300 depends on the amount of signal averaging required to transmit a valid and robust selection. Fig. Figure 5
301 shows the performance curves for varying intensification sequences for the subjects included in the
302 dataset of ALS patients. It can be noticed that the percentage of correctly identified letters depends
303 on the number of intensification sequences k_a that are used to obtain the averaged signal. Moreover,
304 when the number of intensification sequences tend to 1, which corresponds to single-trial letter
305 identification single-intensification character recognition, the performance is reduced. As mentioned before,
306 the SNR of the single-trial P300 obtained from only one segment of the intensification sequence is very
307 low and the shape of its P300 component is not very well defined.

308 In Table ??-3 results obtained for 8 healthy subjects are shown. The obtained performance were slightly
309 inferior than those obtained for ALS patients but well above chance level.

310 In Tables 1 and 3 results for character recognition rates using single channel signals with the
311 SVM (?) classifier and using a feature based on Permutation Entropy and classified by SVM (PE+SVM)
312 are also shown. The PE algorithm, which is also devised on a time-domain description of the waveform,
313 was implemented according to ? and its parameters were adjusted as stated by ?, with an order of 2 and a
314 sliding window of size 10. The SVM classifier, on the other hand, was configured to use a linear kernel.

315 Moreover, Tables 2 and 4 are presented in order to compare the performance of the Histogram of
316 Gradient Orientations (HIST) method against a feature formed by concatenating all the channels (?) and
317 the classification algorithm SWLDA, the methodology proposed by the ALS dataset's publisher. Since
318 authors ? did not report the Character Recognition Rate obtained for this dataset, we replicate their
319 procedure and include the performance obtained with the SWLDA algorithm at letter identification. The
320 obtained performance is improved in 6 out 8 subjects for both datasets.

321 The P300 ERP consists of two overlapping components: the P3a and P3b, the former with frontocentral
322 distribution while the later stronger on centroparietal region (?). Hence, the standard practice is to find
323 the stronger response on the central channel Cz (?). However, ? show that the response may also arise in
324 occipital regions. We found that by analyzing only the waveforms, occipital channels PO8 and PO7 show
325 higher performances for some subjects.

326 As subjects have varying *latencies* and *amplitudes* of their P300 components, they also have a varying
327 stability of the *shape* of the generated ERP (?). Figure 6 shows the 10 sample P300 templates patches
328 for patients 8 and 3 from the dataset of ALS patients. It can be discerned that in coincidence with the
329 performance results, the P300 signature is more clear and consistent for subject 8 (A) while for subject 3
330 (B) the characteristic pattern is more difficult to perceive.

331 Additionally, the stability of the P300 component waveform has been extensively studied in patients
332 with ALS (?????) where it was found that these patients have a stable P300 component, which were also
333 sustained across different sessions. In line with these results we do not find evidence of a difference in
334 terms of the performance obtained for the group of patients with ALS and the healthy group of volunteers.
335 Particularly, the best performance is obtained for a subject from the ALS dataset for which, based on visual
336 observation, the shape of they P300 component is consistently identified.

337 It is important to remark that when applied to binary images obtained from signal plots, the feature
338 extraction method described in Section 2.1.3 generates sparse descriptors. Under this subspace we found
339 that using the cosine metric yielded a significant performance improvement. On the other hand, the unary
340 classification scheme based on the NBNN algorithm proved very beneficial for the P300 Speller Matrix.
341 This is due to the fact that this approach solves the unbalance dataset problem which is inherent to the
342 oddball paradigm (?).

4 DISCUSSION

343 Among other applications of Brain Computer Interfaces, the goal of the discipline is to provide
344 communication assistance to people affected by neuro-degenerative diseases, who are the most likely
345 population to benefit from BCI systems and EEG processing and analysis.

346 In this work, a method to detect transient P300 components from EEG signals based on their waveform
347 characterization in digital time-space, is presented. Additionally, its validity is evaluated using a public
348 dataset of ALS patients and an own dataset of healthy subjects.

349 ~~This method has the~~ It was verified that this method has an improved performance at letter identification
350 than other methods that process the signals on a channel by channel strategy, and it even has a slightly
351 improved performance compared to other methods like SWLDA, which uses a multichannel feature.
352 Furthermore, this method has the advantage that shapes of waveforms can be analyzed in an objective
353 way. We observed that the shape of the P300 component is more stable in occipital channels, where
354 the performance for identifying letters is higher. We additionally verified that ALS P300 signatures are
355 stable in comparison to those of healthy subjects. Further work should be conducted over larger samples
356 to cross-check the validity of these results.

357 We believe that the use of descriptors based on histogram of gradient orientation, presented in this work,
358 can also be utilized for deriving a shape metric in the space of the P300 signals which can complement
359 other metrics based on time-domain as those defined by ?. It is important to notice that the analysis of
360 waveform shapes is usually performed in a qualitative approach based on visual inspection (?), and
361 a complementary methodology which offer a quantitative metric will be beneficial to these routinely
362 analysis of the waveform of ERPs.

363 The goal of this work is to answer the question if a P300 component could be solely determined by
364 inspecting automatically their waveforms. We conclude affirmatively, though two very important issues
365 still remain:

366 First, the stability of the P300 in terms of its shape is crucial: the averaging procedure, montages, the
367 signal to noise ratio and spatial filters all of them are non-physiological factors that affect the stability of
368 the shape of the P300 ERP. We tested a preliminary approach to assess if the morphological shape of the
369 P300 of the averaged signal can be stabilized by applying different ~~latency shifts to segments alignments~~
370 of the stacked segments (see Figure 2) and we verified that there is a better performance when a correct
371 ~~single-trial segment~~ alignment is applied. We also applied Dynamic Time Warping (DTW) (?) to automate
372 the alignment procedure but we were unable to find a substantial improvement. Further work to study the
373 stability of the P300 signature component needs to be addressed.

374 The second problem is the amplitude variation of the P300. We propose a solution by standardizing
375 the signal, shown in Eq. 2. It has the effect of normalizing the peak-to-peak amplitude, moderating its
376 variation. It has also the advantage of reducing noise that was not reduced by the averaging procedure. It

377 is important to remark that the averaged signal variance depends on the number of **single-trials**-segments
378 used to compute it (?). The standardizing process converts the signal to unit signal variance which makes it
379 independent of the number k_a of signals averaged. Although this is initially an advantageous approach, the
380 standardizing process reduces the amplitude of any significant P300 complex diminishing its automatic
381 interpretation capability.

382 In our opinion, the best benefit of the presented method is that a closer collaboration with physicians can
383 be fostered, since this procedure intent to imitate human visual observation. Automatic classification of
384 patterns in EEG that are specifically identified by their shapes like K-Complex, Vertex Waves, Positive
385 Occipital Sharp Transient (?) are a prospect future work to be considered. We are currently working
386 in unpublished material analyzing **KComplex-K-Complex components** that could eventually provide
387 assistance to physicians to locate these EEG patterns, specially in long recording periods, frequent in
388 sleep research. Additionally, it can be used for artifact removal which is performed on many occasions
389 by visually inspecting signals. This is due to the fact that the descriptors are a direct representation of
390 the shape of signal waveforms. In line with these applications, it can be used to build a database (?) of
391 quantitative representations of waveforms and improve atlases (?), which are currently based on qualitative
392 descriptions of signal shapes.

CONFLICT OF INTEREST STATEMENT

393 The authors declare that the research was conducted in the absence of any commercial or financial
394 relationships that could be construed as a potential conflict of interest.

AUTHOR CONTRIBUTIONS

395 This work is part of the PhD thesis of RR which is directed by JS and codirected by AV.

FUNDING

396 This project was supported by the ITBACyT-15 funding program issued by ITBA University from Buenos
397 Aires, Argentina.

ACKNOWLEDGMENTS

398 We would like to thank to Dr. Valentina Unakafova for providing the Permutation Entropy algorithm.

Table 1. Percentage of correctly predicted letters Character recognition rates while performing an offline BCI Simulation for the best performing channel for each subject of the public dataset of ALS patients using the Histogram of Gradients (HIST). The spelled words are *GATTO*, *MENTE*, *VIOLA* and *REBUS*. Performance rates and the best performing channel with the SVM classifier and, using a feature obtained with Permutation Entropy (PE) and classified by SVM, are also shown for comparison.

Participant	BPC	HIST	Performance	BPC	SVM	BPC	PE+SVM
1	Cz	35%		Cz	15%	P3	5%
2	Fz	85%		PO8	25%	PO8	15%
3	Cz	25%		Fz	5%	P3	5%
4	PO8	55%		Oz	5%	Oz	10%
5	PO7	40%		P3	25%	PO8	15%
6	PO7	60%		PO8	20%	Fz	10%
7	PO8	80%		Fz	30%	Fz	10%
8	PO7	95%		PO7	85%	PO8	25%

Table 2. Percentage of correctly predicted letters while performing an offline BCI Simulation Character recognition rates for the best performing channel for each subject public dataset of ALS patients using the own dataset. The spelled words are *MANSO*, *CINCO*, *JUEGO* Histogram of Gradient (HIST) and *QUESO* performance rates obtained by the SWLDA with a multichannel concatenated feature.

Participant	BPC	Performance	HIST	SWLDA
1	Cz	35%		45%
2	Fz	85%		30%
3	Cz	25%		65%
4	PO8	55%		40%
5	PO7	40%		35%
6	PO7	60%		35%
7	PO8	80%		60%
8	PO7	95%		90%

Table 3. Percentage of correctly predicted letters while performing an offline BCI Simulation for the best performing channel for each subject of the own dataset. The spelled words are *MANSO*, *CINCO*, *JUEGO* and *QUESO*. Performance rates using single channel signals with the SVM classifier and using a feature obtained with Permutation Entropy (PE) and classified by SVM are also shown for comparison.

Participant	BPC	HIST	BPC	SVM	BPC	PE+SVM
1	Oz	40%	Cz	10%	PO7	10%
2	PO7	30%	Cz	5%	Fz	5%
3	P4	40%	P3	10%	Fz	0%
4	P4	45%	P4	35%	Cz	10%
5	P4	60%	P3	10%	Fz	0%
6	Pz	50%	P4	25%	Cz	10%
7	PO7	70%	P3	30%	P3	10%
8	P4	50%	PO7	10%	Fz	5%

Table 4. Percentage of correctly predicted letters while performing an offline BCI Simulation for the best performing channel for each subject of the own dataset. Results obtained with the SWLDA algorithm with a multichannel concatenated feature are presented.

Participant	BPC	HIST	SWLDA
1	Oz	40%	65%
2	PO7	30%	15%
3	P4	40%	50%
4	P4	45%	40%
5	P4	60%	30%
6	Pz	50%	35%
7	PO7	70%	25%
8	P4	50%	35%

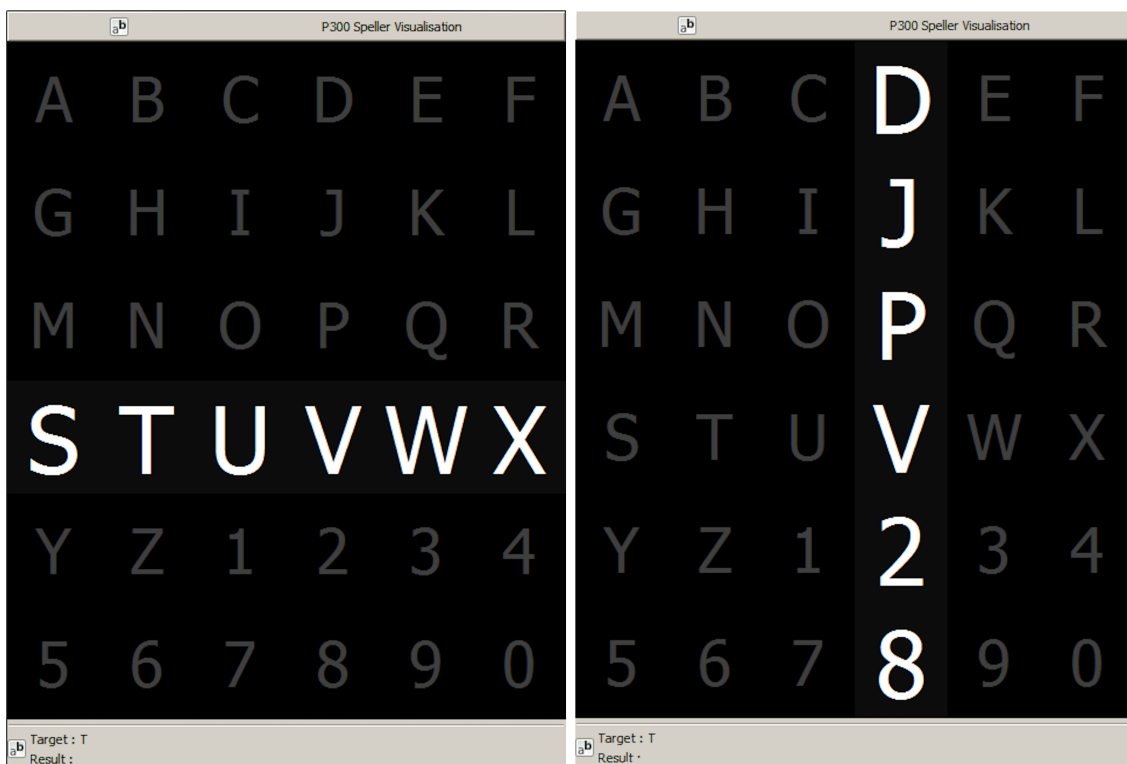


Figure 1. Example of the 6×6 Speller Matrix used in the study [obtained from the OpenVibe software](#). Rows and columns flash **intermittently** in random permutations.

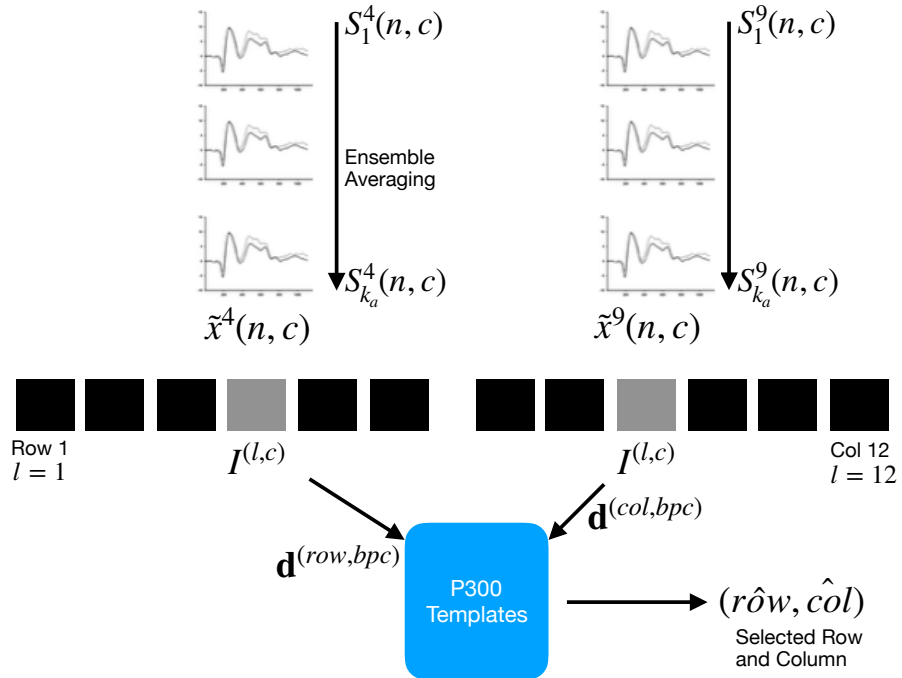


Figure 2. For each column and row, an averaged, standardized and scaled signal $\tilde{x}^l(n, c)$ is obtained from the segments S_i^l corresponding to the k_a intensification sequences with $1 \leq i \leq k_a$ and location l varying between 1 and 12. From the averaged signal, the image $I^{(l,c)}$ of the signal plot is generated and each descriptor is computed. By comparing each descriptor against the set of templates, the P300 ERP can be detected, and finally the desired letter from the matrix can be inferred.

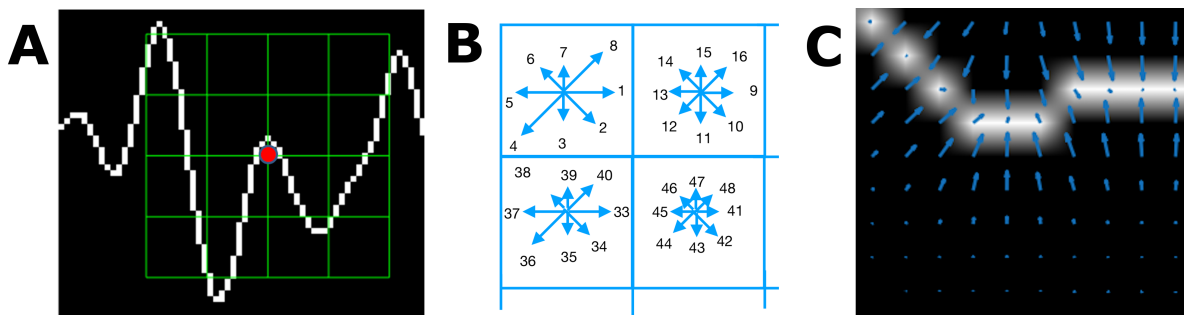


Figure 3. (A) Example of a plot of the signal, a keypoint and the corresponding patch. (B) A scheme of the orientation's histogram computation. Only the upper-left four blocks are visible. The first eight orientations of the first block, are labeled from 1 to 8 clockwise. The orientation of the second block $B_{1,2}$ is labeled from 9 to 16. This labeling continues left-to-right, up-down until the eight orientations for all the sixteen blocks are assigned. They form the corresponding kp-descriptor descriptor of 128 coordinates. The length of each arrow represent the value of the histogram on each direction for each block. (C) Vector field of oriented gradients. Each pixel is assigned an orientation and magnitude calculated using finite differences.

~~Single trial segments S_i are averaged for the 6 rows and 6 columns. From the averaged signal, the image of the signal plot is generated and each descriptor is computed. By comparing each descriptor against the set of templates, the P300 ERP can be detected, and finally the desired letter from the matrix can be inferred.~~

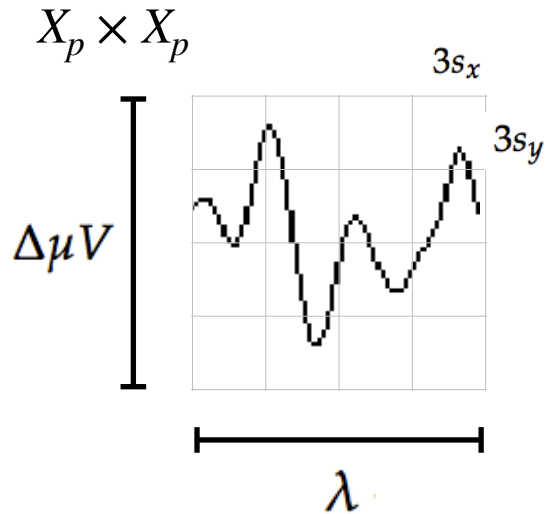


Figure 4. The scale of local patch is selected in order to capture the whole transient event. The size of the patch is $X_p \times X_p$ pixels. The vertical size consists of 4 blocks of size $3s_y$ pixels which is high enough as to contain the signal $\Delta\mu V$, the peak-to-peak amplitude of the transient event. The horizontal size includes 4 blocks of $3s_x$ and covers the entire duration in seconds of the transient signal event, λ .

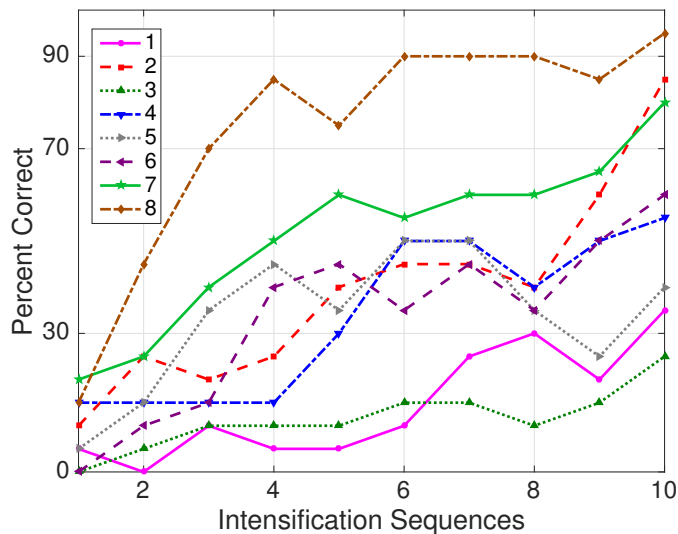


Figure 5. Performance curves for the eight subjects included in the dataset of ALS patients. Three out of eight subjects achieved the necessary performance to implement a valid P300 speller.

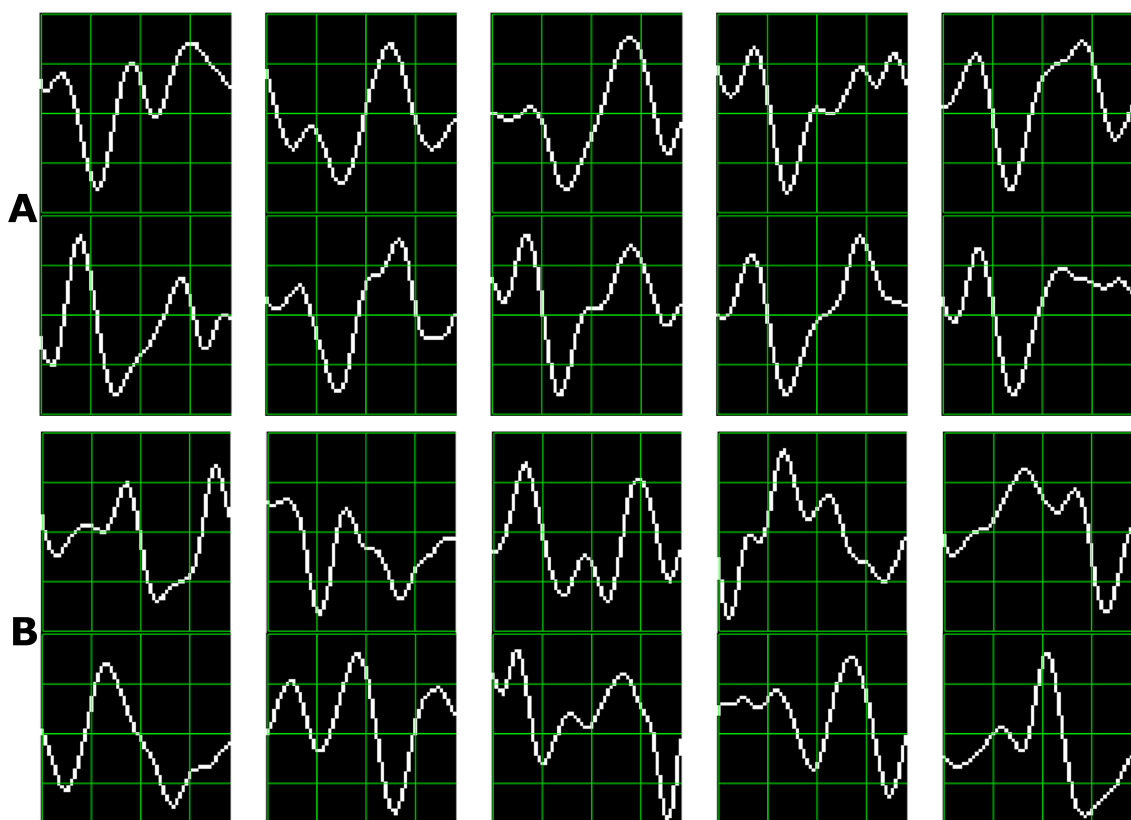


Figure 6. [Ten sample P300 template patches for subjects 8 \(A\) and 3 \(B\) of the ALS Dataset.](#) As traditional done in neuroscience research, [downward](#) [Downward deflection](#) is positive polarity.